Journal of Mineralogical and Petrological Sciences, Volume 110, page 76–81, 2015

LETTER

Ruby-bearing feldspathic dike in peridotite from Ray-Iz ophiolite, the Polar Urals: Implications for mantle metasomatism and origin of ruby

Satoko ISHIMARU[*], Shoji ARAI[**,***], Makoto MIURA[**], Vladimir R. SHMELEV[†] and Evgeny PUSHKAREV[†]

[*]*Department of Earth and Environmental Sciences, Graduate School of Science and Technology, Kumamoto University, 2-39-1 Kurokami, Chuo-ku, Kumamoto 860-8555, Japan*
[**]*Department of Earth Sciences, Kanazawa University, Kakuma, Kanazawa 920-1192, Japan*
[***]*ODS, JAMSTEC, 2-15 Natsushima, Yokosuka 237-0061, Japan*
[†]*Zavaritskii Institute of Geology and Geochemistry, Ural Branch, Russian Academy of Sciences, Russia*

Crystallization of ruby requires excess Al and appreciable amounts of Cr in the system. A ruby-bearing feldspathic dike crosscuts dunite in the Ray-Iz massif, the Polar Urals, and the dominant mineral of the dike changes from plagioclase at the center to amphibole outward. Ruby has been observed in between, and the zone is composed of plagioclase and phlogopite with minor chromian spinel and ruby as primary phases, and paragonite as a secondary phase. The Cr_2O_3 content of the ruby is <7.5 wt% and close to the values of those found in serpentinite and chromitite from other localities. The petrographical and highly LREE-enriched and HREE-depleted features of the ruby-bearing rock imply a metasomatic origin for the dike through the interaction between feldspathic component-rich aqueous fluid and wall rock dunite with chromitite. Based on the primary occurrence of plagioclase, it is inferred that the fluid infiltration possibly occurred at 1.0–1.5 GPa, and the fluid interacts with peridotite. The lithological change of the dike indicates effective consumption of Si, Ca, and K and assimilation of Cr and Mg in the fluid at the contact with the wall-rock dunite, and the fluid composition could have evolved to be peraluminous through the interaction. Chromium is effectively transported by aqueous fluid with some anions, e.g., Cl^-, CO_3^{2-}, and SO_3^{2-}, and the interaction of peridotite as a source of Cr with such fluids is one of the important formation processes of ruby within the mantle wedge where fluids are available from the downgoing slab.

Keywords: Feldspathic dike, Ruby, Metasomatism, Ray-Iz ophiolite

INTRODUCTION

Corundum occurs in a wide variety of rocks: igneous, metamorphic, sedimentary, and extraterrestrial (e.g., Simonet et al., 2008). Their occurrences largely depend on the availability of excess Al, and other factors such as pressure and temperature are less important (e.g., Simonet et al., 2008). Ruby is one variety of corundum, and contains appreciable amounts of Cr. Therefore, the Cr-rich peraluminous condition is indispensable for its crystallization, and the upper mantle rocks, in situ or emplaced in the crust, are suitable for ruby crystallization when Al-rich melts or fluids are available. The most Cr-rich ruby (12.9 wt% Cr_2O_3), showing deep reddish tints, has been reported from a serpentinite-derived metasomatic rock from New Zealand (Grapes and Palmer, 1996).

Very few works have referred to the formation of ruby as a mantle metasomatic process. In addition, the optimum condition for ruby formation is still unclear, although many gemologists have been interested in its production (e.g., Simonet et al., 2008). There is a report of a ruby-bearing feldspathic dike in dunite in the mantle section of the Ray-Iz ophiolite, and the petrographic features imply their metasomatic origin (Scherbakova, 1975). Here, we present the detailed petrographic and geochemical characteristics of the ruby-bearing feldspathic dike, and discuss its petrogenesis. The formation of ruby there possibly mimics a type of mantle metasomatism by high-Al fluids or melts, and provides implications for the be-

doi:10.2465/jmps.141021
S. Ishimaru, ishimaru@sci.kumamoto-u.ac.jp Corresponding author

havior of Cr during metasomatism.

GEOLOGICAL BACKGROUND

The Ural Mountains represent a linear mid-Paleozoic orogenic zone formed during the closure of an ocean basin-island arc system between the European Plate to the west and the Siberian Plate to the east (e.g., Brown et al., 2006). In the Polar Urals, a long ophiolitic belt comprises three massifs, the Voykar, Syum-Keu, and Ray-Iz, which are separated from one another by a Precambrian metamorphic formation (e.g., Shmelev et al., 2014). The Ray-Iz ophiolite, 400 km^2 in area, is thrust over the Paleozoic sedimentary rocks of the East European Platform (Shmelev et al., 2014). Its mantle tectonite has been changed to metaperidotite, and varies from lherzolite-harzburgite to harzburgite-dunite (Shmelev, 2011). An apparent Moho transition zone is located at the southern end of the ophiolite, and is bounded by the peridotite tectonite and Moho transition zone with faults (Shmelev et al., 2014). Recent detailed petrographical and geochemical works support a supra-subduction zone origin for the Ray-Iz ophiolite (e.g., Shmelev, 2011): the harzburgite-dominant lithology of the mantle section, large-scale chromite ore mineralization, and enrichment of Cs, Rb, and Ba in volcanic rocks relative to N-MORB.

Although we did not observe any field occurrence of the ruby-bearing dike, Scherbakova (1975) described the dike and the surrounding peridotite in detail before the backfill. She recognized two types of ruby-bearing dikes, 1) plagioclase-rich, and 2) phlogopite-rich, but we only obtained samples of the former from creek boulders. The ruby-bearing plagioclase-rich dike (320 ± 20 Ma; Makeyev, 2006) was about 10-12 m in width and showed clear symmetrical zoning (Scherbakova, 1975) (Fig. 1). The mineral assemblage changes from almost plagioclase (andesine to oligoclase) rock at the center to an outer zone rich in amphibole (tremolite-actinolite), chromian spinel, and clinochlore, through a zone rich in ruby, phlogopite, and chromian spinel (Scherbakova, 1975) (Fig. 1). The volume of plagioclase in the dike decreases from 95% in the central part to 1% in the outer part (Scherbakova, 1975). The 0.3-1.0 m wide ruby-bearing zone (Fig. 1) is further subdivided into two (inner phlogopite-rich and outer phlogopite and plagioclase-rich) parts, and ruby is relatively abundant in the outer parts (Scherbakova, 1975). The wall serpentinized dunite also shows a change of mineral assemblage (Fig. 1); kämmererite- and talc-bearing chromian spinel-rich zone was observed along both sides of the contact (Scherbakova, 1975). Chromian spinel is absent in the central part of the dike, and appears in a mica-rich zone, especially around ruby, and the modal amount of chromian spinel reaches a maximum at the contact with serpentinized dunite (Scherbakova, 1975).

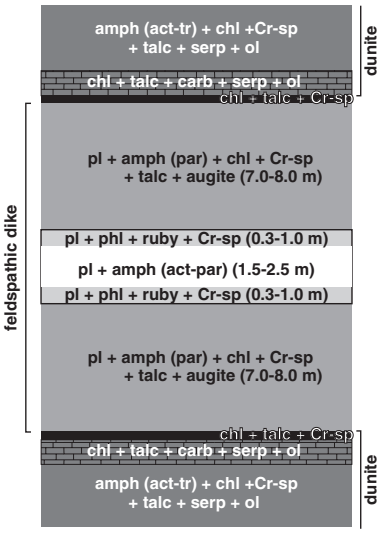

Figure 1. Schematic image showing relationship between the feldspathic dike in Ray-Iz dunite. This image is based on the description by Scherbakova (1975). Order of minerals in each part does not represent their modal abundances (see text).

PETROGRAPHY OF RUBY-BEARING SAMPLES

The mineral assemblage of the ruby-bearing sample (Fig. 1) is plagioclase, phlogopite, paragonite, and chromian spinel with or without zoisite (Figs. 2a-2c), which is slightly different from the description of Scherbakova (1975). Phlogopite is elongated in shape and strongly pleochroic (yellowish brown to almost colorless) in feature (Fig. 2d). Chromian spinel varies in shape from coarse (more than 1 cm) subhedral to anhedral (Fig. 2e) to fine (less than 100 μm) elongated and/or euhedral to subhedral (Figs. 2d-2g). Ruby shows pinkish to reddish colors and anhedral shapes (Figs. 2f and 2g). Paragonite occasionally shows a bluish color, surrounding ruby and enclosing fine (<5 μm) chromian spinel (Figs. 2f and 2g), and is completely absent in ruby-free parts (Fig. 2d). Ruby is never in direct contact with plagioclase; paragonite always occurs between ruby and plagioclase (Figs. 2f and 2g). Margarite is also observed as a thin layer in paragonite at the contact with ruby. Although variable in modal compositions (Figs. 2a-2c), the most predominant phase is plagioclase (32-67 vol%), followed by paragonite (7-31 vol%) and phlogopite (10-22 vol%). The chromian spinel content is almost constant (5-7 vol%) but abundant (≤15 vol%) in some samples (e.g., RY09-6: Fig. 2b). It is noteworthy that fine subhedral to euhedral chromian spinel grains are enclosed in all the other minerals (phlogopite, plagioclase, paragonite, and ruby).

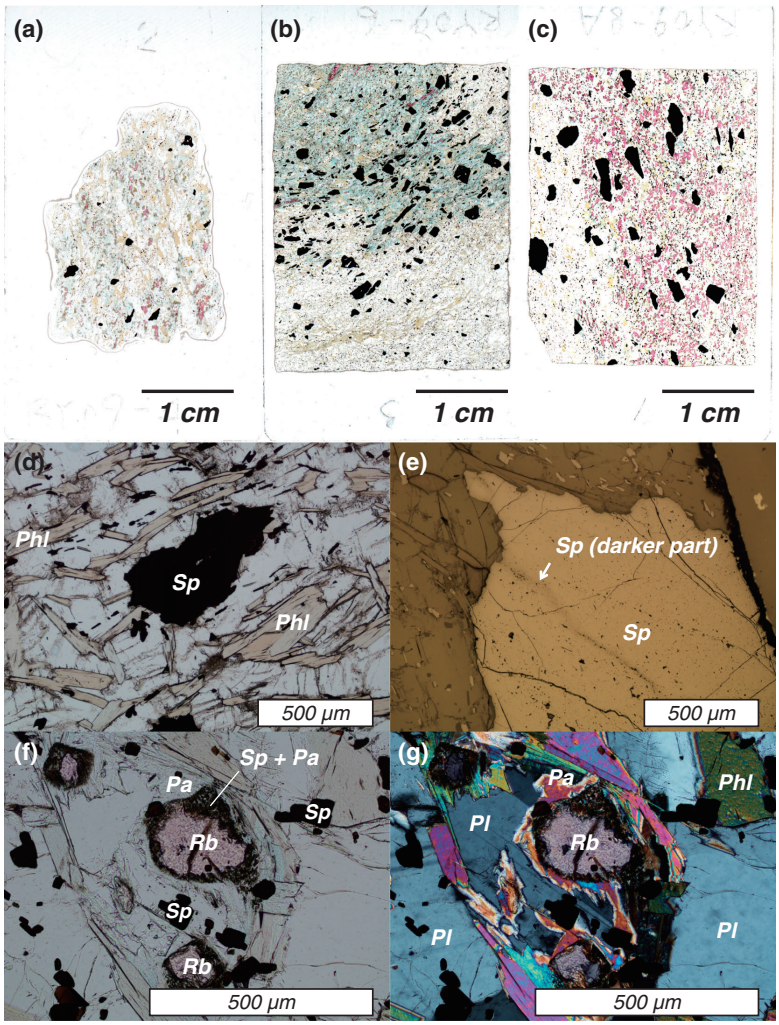

Figure 2. Worked scanned image of thin sections of the ruby-bearing feldspathic rock (a) to (c) and photomicrographs showing specific petrographic features of the feldspathic rocks from (d) to (g). Abbreviations are as follows: Sp, chromian spinel; Phl, phlogopite; Rb, ruby; Pa, paragonite; Pl, plagioclase. (a) PPL image of RY09-4. Yellowish, bluish, black, and pinkish minerals are phlogopite, paragonite, chromian spinel, and ruby, respectively. (b) PPL image of RY09-6. Greenish part is quite rich in paragonite. (c) PPL image of RY09-8A. This sample contains a high amount of ruby (~ 16 vol%). (d) PPL image of ruby-free part of the feldspathic dike. Paragonite is also absent. (e) Reflected light image of coarse chromian spinel showing darker rim and vein-like part. (f) Ruby-bearing part of the feldspathic dike. Fine chromian spinel grains show euhedral to subhedral shapes. Ruby partly changes to mineral assemblage of fine chromian spinel and paragonite. (g) XPL image of (f). Note that there is always paragonite between plagioclase and ruby.

Chromian spinel itself occasionally encloses other minerals (K phlogopite, plagioclase, and Na phlogopite) when coarse in size, and Na phlogopite coexists with K phlogopite, when there is any (Table 1). Euhedral chromian spinel is not associated with ruby (Scherbakova, 1975) except in fine-grained aggregates with paragonite (Figs. 2d, 2f, and 2g). Fluid inclusions are occasionally observed in plagioclase.

ANALYTICAL METHODS

For bulk-rock analyses, we made fused whole-rock glass discs using a direct fusion method (Nicholls, 1974). Details of our analyses are described in Ichiyama et al. (2013). Major-element contents were determined using FE-SEM (JSM-7001F, JEOL) with an EDS system (INCA energy, Oxford Instruments) at Kumamoto University. The accelerating voltage, probe current, and probe diameter were 15 kV, 1 nA, and <1 μm, respectively, for the EDS analysis. Trace-element contents were determined using laser ablation (193 nm ArF excimer: MicroLas GeoLas Q-Plus) inductively coupled plasma mass spectrometry (Agilent 7500s, Yokogawa Analytical Systems) at Kanazawa University. LA-ICPMS analyses were performed by 100 μm and 60 μm diameter spots on fused glass and minerals, respectively, at a repetition rate of 6 Hz with an energy density of 8 J/cm^2 per pulse. BCR-2G and NIST 612 glass was used as an external calibration standard for fused glass and minerals, respectively. Analytical details can be found in Morishita et al. (2005).

GEOCHEMICAL FEATURES OF THE DIKE

Major-element compositions of the ruby-bearing rock are characterized by high Al_2O_3 (~ 36 wt%) and Cr_2O_3 (~ 2.4 wt%) contents and low contents of SiO_2 (~ 43 wt%), FeO* (6.4 wt%), MgO (~ 4 wt%), and CaO (~ 3.4 wt%) on an anhydrous basis. The rock shows unusual CIPW norm compositions, containing 24% corundum,

Table 1. Representative mineral compositions of feldspathic dike

Sample No.	RY09-6										RY09-4	
	2-sp1-1 coarse-c	2-sp1-2 coarse-r	8-sp1 fine	5-pl1	7-Kfeld1	2-phl1	2-phl2-1 in sp	2-phl2-2 in sp	5-wm1 paragonite	7-wm1 margarite	4-rb1	7-rb1-1
SiO_2	0.00	0.00	0.00	59.24	66.52	37.45	37.87	38.90	40.52	30.81		
TiO_2	0.00	0.00	0.00		0.28	0.85	1.23	0.56				
Al_2O_3	10.81	21.71	26.64	25.22	17.53	21.02	20.12	21.58	41.60	46.36	95.16	89.53
Cr_2O_3	55.04	43.43	38.09			2.06	2.08	2.73	0.65	1.19	3.86	7.53
Fe_2O_3	1.46	1.59	1.58									
FeO	26.48	24.64	24.93			3.69	3.29	2.69	0.32	0.30	0.44	
MnO	1.09	0.95	0.64									0.84
MgO	4.38	6.68	7.05			19.87	19.54	20.48	0.59	0.85		
CaO	0.00	0.00	0.00	6.48					2.22	8.95		
Na_2O	0.00	0.00	0.00	7.88		1.52	1.84	6.49	5.23	1.86		
K_2O	0.00	0.00	0.00		14.40	7.80	7.00	0.42	0.19			
NiO	0.00	0.00	0.00									
Total	99.26	99.00	98.93	98.82	98.73	94.26	92.97	93.85	91.32	90.32	99.46	97.90
Mg#	0.228	0.326	0.335			0.906	0.914	0.931				
Cr#	0.774	0.573	0.490									
Na/(Na+Ca)				0.312					0.810	0.273		
Na/(Na+K)						0.228	0.285	0.959				
Y(Cr)	0.759	0.562	0.480									
Y(Al)	0.222	0.419	0.501									
Y(Fe)	0.019	0.020	0.019									

Calculation of ferric and ferrous iron in chromian spinel is based on the stoichiometry. Mg#, Mg/(Mg + Fe total) atomic ratio and Mg/(Mg + Fe^{2+}) atomic ratio for silicates and chromian spinel, respectively. Cr#, Cr/(Cr + Al) atomic ratio. Y(Al), Al/(Al + Cr + Fe^{3+}) atomic ratio. Y(Cr), Cr/(Al + Cr + Fe^{3+}) atomic ratio. Y(Fe), Fe^{3+}/(Al + Cr + Fe^{3+}) atomic ratio. 2-sp1-1 and 2-sp1-2 represent data for the core and rim, respectively, of one coarse chromian spinel grain. 2-phl2-1 and 2-phl2-2 coexist in a single inclusion of a chromian spinel grain.

4% chromite, and 49% feldspars if we assume a ferric iron to total iron ratio of 0.2.

The bulk-rock REE pattern, normalized to C1 chondrite values (Sun and McDonough, 1989), shows an LREE-rich and HREE-depleted character with a positive Eu spike (Fig. 3a). The chondrite-normalized incompatible trace-element pattern shows strong positive anomalies at Ba and Sr, and a negative anomaly at Zr (Fig. 3b).

The samples show correlations between bulk major-element compositions and modal proportions of minerals. Plagioclase varies from An_{25} to An_{35} (oligoclase to andesine) with very low K_2O (almost below the detection limit) (Table 1). Na_2O and CaO in all K-feldspars are below their detection limits. All phlogopites, except inclusions in coarse chromian spinel, show high Mg# (0.89-0.95), K-rich features [Na/(Na + K) atomic ratio = 0.16-0.35], and almost constant TiO_2 contents (0.5-1.7 wt%) (Table 1). The Na phlogopite (2-phl2-2 in Table 1) in chromian spinel shows a high Na/(Na + K) atomic ratio (0.96) with high Mg# (0.93), and the coexisting K-rich phlogopite shows similar Na/(Na + K) (0.29; 2-phl2-1 in Table 1) to discrete grains of K phlogopite (0.23) (2-phl1 in Table 1). Paragonite shows almost constant Na/(Na + Ca) atomic ratios (~ 0.8) with some exceptions (Table 1). The Na/(Na + Ca) atomic ratio of the margarite layer in paragonite is 0.3 (Table 1). Both paragonite and margarite contain high Cr_2O_3 (0.3-2.3 wt% and 1.2-1.4 wt%, respectively) (Table 1). Ruby contains 0.3 to 7.5 wt% Cr_2O_3 and minor amounts of FeO* (0.3-0.5 wt%). Some ruby grains show chemical zoning, the core containing highest Cr_2O_3 (7.5 wt%), and the rim containing lower Cr_2O_3 (4.4 wt%). Coarse chromian spinel grains show higher Cr# [= Cr/(Cr + Al) atomic ratio] at the core (0.74-0.86) than at the rim (0.46-0.63) (Table 1). Fine (mostly <100 μm across) chromian spinel grains are homogeneous in Cr# (0.46-0.64), almost equal to the coarse grain rim value (Table 1). The Mg# [= Mg/(Mg + Fe^{2+}) atomic ratio] of chromian spinel is 0.21-0.31 at the core of coarse grains, 0.32-0.40 at the rim of coarse grains, and 0.26-0.41 on fine grains. The ferric iron ratio to the trivalent cations in chromian spinel is almost constant, irrespective of grain size (≈ 0.01-0.03). The coarse chromian spinel is similar in Cr# to those in surrounding Ray-Iz dunite and/or chromitite (0.7-0.8; Miura et al., unpublished data 2014).

Plagioclase shows highly LREE-enriched patterns, and some MREE and HREE were not detected (Fig.

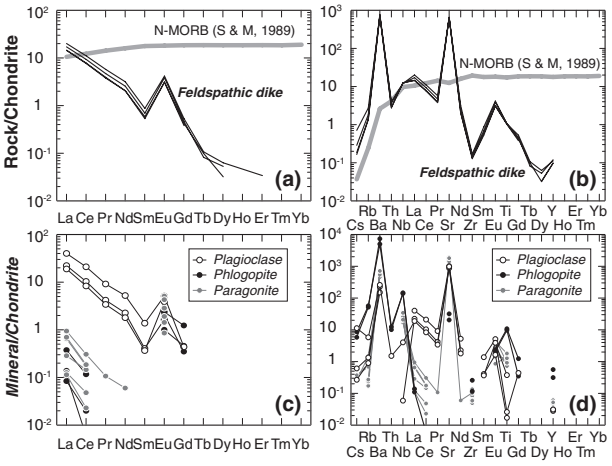

Figure 3. REE and incompatible trace-element patterns, normalized to C1 chondrite values (Sun and McDonough, 1989), for bulk rock (a), (b) and minerals (c), (d). Thick gray patterns in panel (a), (b) indicate N-MORB values (Sun and McDonough, 1989) for reference.

3c). Only some LREE are detectable for micas, K phlogopite, and paragonite, possibly with a positive Eu spike (Fig. 3c). All analyzed minerals show extremely high positive spikes at Ba and Sr in chondrite-normalized patterns with high concentrations of other LILE (Cs and Rb) (Fig. 3d). Trace-element patterns of phlogopite show positive anomalies at Nb and Ti as well (Fig. 3d).

DISCUSSIONS AND IMPLICATIONS

Petrographical and geochemical features of the ruby-bearing feldspathic dike indicate that their primary mineral assemblage was plagioclase, phlogopite, chromian spinel, and ruby. Paragonite, which is large in modal abundance (Fig. 2), is of secondary origin, formed by the reaction between the primary ruby and plagioclase (Figs. 2f and 2g). This is consistent with the absence of paragonite when ruby is absent (Figs. 2b and 2d). Generally, corundum will react with plagioclase to form white mica at low temperatures (T ~ 580-700 °C) under hydrous conditions at P = 0.5 GPa (e.g., Ackermand and Morteani, 1973). In the present case, the ruby has been texturally replaced by paragonite and flaky chromian spinel. Paragonite inherited the high Cr character from ruby (up to 2.3 wt% Cr_2O_3). The strong enrichment of Ba and Sr in paragonite is also inherited from a primary plagioclase characteristic (Fig. 3). The rare margarite possibly formed in the same manner as paragonite, at lower temperature (T ~ 580 °C; Ackermand and Morteani, 1973). The pressure for the dike formation was possible lower than 1.0-1.5 GPa because of crystallization of primary plagioclase (≈ An_{30}) in equilibrium with olivine and chromian spinel (e.g., Borghini et al., 2011). Paragonite and minor margarite appeared by retrogressive reaction between ruby and plagioclase, possibly during the exhumation stage of the Ray-Iz ophiolite. The dike was probably formed by crystallization of melt or fluid rich in feldspar components, combined with reaction with the wall rock (dunite with chromitite; Shmelev et al., 2014). If our ruby-bearing rock is of metamorphic origin, i.e., broken down from a higher-pressure rock, paragonite should be in equilibrium with corundum, and symplectic textures would have appeared (e.g., Tropper and Manning, 2004). However, the texture and high-Cr character of paragonite deny their simultaneous crystallization. In addition, retrogressive recrystallization could not form the gradual lithological change across the dike (Fig. 1).

It is very possible that the melt or fluid acquired a peraluminous character by precipitation of relatively Al-poor or Al-free minerals along the wall. The zonal distribution of minerals in the feldspathic dike (Fig. 1) implies that the amphibole-rich part is a reaction zone between the melt/fluid and wall rock, which changed the chemistry of the involved melt/fluid by consumption of SiO_2 and CaO, combined with a gain in MgO, FeO, and Cr_2O_3. The formation of talc in the wall-rock dunite may also reflect SiO_2 addition from the melt/fluid (Fig. 1). In this context, we suggest that the central part of the dike was precipitated from the intact part of the melt/fluid. These relationships have also been reported from a sapphirine-bearing vein and host peridotite in the Finero phlogopite-peridotite massif (Giovanardi et al., 2013).

Our ruby-bearing rock shows an LREE-enriched pattern [$(La/Sm)_{CN}$ ~ 24] with strong positive anomalies at Ba and Sr (Fig. 3). This characteristic is due to the abundance of primary plagioclase, and was not changed during the formation of paragonite (Fig. 3). The ruby-bearing feldspathic rock is distinctly different in trace-element character from a plagiogranite formed by melting of basaltic rock, which shows a much flatter REE pattern [$(La/Sm)_{CN}$ = 0.4-1.7] (Gerlach et al., 1981). This indicates that the melt or fluid involved was highly evolved silicate magma or aqueous fluid with high $(La/Sm)_{CN}$ (e.g., Bizimis et al., 2000), possibly rich in plagioclase component. We prefer fluid to melt as an agent for the dike formation, because of the presence of fine euhedral chromian spinel, indicating the Cr-rich character of the high-Al agent. The solubility of Cr in silicic melts is very low (e.g., Irvine, 1977), but high-T aqueous fluids can dissolve appreciable amounts of Cr to precipitate chromian spinel (e.g., Arai and Akizawa, 2014). The coarse chromian spinel, with a high Cr# core and low Cr# rims (Table 1), are of xenocrystal origin from the wall dunite and/or chromitite. Therefore, the primary fluid infiltrated

was possibly silicic and aluminous, and highly reactive with peridotite (or chromitite) to precipitate a large amount of amphiboles; the wall dunite and chromitite was an essential host for desilication of the fluid (Simonet et al., 2008). The fluid incorporated an appreciable amount of Cr from chromian spinel grains trapped by the wall.

The occurrence of ruby in the mantle section of the supra-subduction-origin Ray-Iz ophiolite indicates that the ruby-forming metasomatism is available in the mantle wedge, where aqueous fluids rich in Al and Si are supplied from the slab. Peridotites and chromitites with high-Cr# spinels are very common in the mantle wedge (e.g., Ishimaru et al., 2007), and will serve as a desilication agent, resulting in excess-Al characteristics in the fluid involved. Plagioclase occasionally contains fluid inclusions, of which the main components are HCO_3^-, SO_4^{2-}, and Cl^- (Scherbakova, 1975). Rubies may be effectively formed within the fluid metasomatic processes because the fluids with appreciable Cl^-, CO_3^{2-}, and SO_3^{2-} are capable of dissolving Cr^{3+} from chromian spinel (Arai and Akizawa, 2014).

ACKNOWLEDGMENTS

Comments from M. Obata, an associate editor, an anonymous reviewer, and T. Morishita were instructive in improving the manuscript. T. Hasenaka, F. Sugiyama, Y. Hirakawa, Y. Kusano, and A. Tamura helped us greatly in the analysis. This work is partly supported by Grant-in-Aid for Scientific Research (C) (24540518) to SI.

REFERENCES

Ackermand, D. and Morteani, G. (1973) Occurrence and breakdown of paragonite and margarite in the Greiner Schiefer series (Zillerthal Alps, Tyrol). Contributions to Mineralogy and Petrology, 40, 293-304.

Arai, S. and Akizawa, N. (2014) Precipitation and dissolution of chromite by hydrothermal solutions in the Oman ophiolite; New behavior of Cr and chromite. American Mineralogist, 99, 28-34.

Bizimis, M., Salters, V.J. and Bonatti, E. (2000) Trace and REE content of clinopyroxenes from supra-subduction zone peridotites. Implications for melting and enrichment processes in island arcs. Chemical Geology, 165, 67-85.

Borghini, G., Fumagalli, P. and Rampone, E. (2011) The geometric significance of plagioclase in mantle peridotites: A link between nature and experiments. Lithos, 126, 42-53.

Brown, D., Spadea, P., Puchkov, V., Alvarez-Marron, J., Herrington, R., Willner, A.P., Hetzel, R., Gorozhanina, Y. and Juhlin, C. (2006) Arc-continent collision in the Southern Urals. Earth-Science Reviews, 79, 261-287.

Gerlach, D.C., Leeman, W.P. and Avé Lallemant, H.G. (1981) Petrology and geochemistry of plagiogranite in the Canyon Mountain ophiolite, Oregon. Contributions to Mineralogy and Petrology, 77, 82-92.

Giovanardi, T., Morishita, T., Zanetti, A., Mazzucchelli, M. and Vannucci, R. (2013) Igneous sappirine as a product of melt-peridotite interactions in the Finero phlogopite-peridotite massif, Western Italian Alps. European Journal of Mineralogy, 25, 17-31.

Grapes, R. and Palmer, K. (1996) (Ruby-sapphire)-chromian mica- tourmaline rocks from Westland, New Zaeland. Journal of Petrology, 37, 293-315.

Ichiyama, Y., Morishita, M., Tamura, A. and Arai, S. (2013) Petrology of peridotite xenolith-bearing basaltic to andesitic lavas from the Shiribeshi Seamount, off northwestern Hokkaido, the Sea of Japan. Journal of Asian Earth Sciences 76, 48-58.

Irvine, T.N. (1977) Origin of chromitite layers in the Muskox intrusion and other stratiform intrusions: A new interpretation. Geology, 5, 273-277.

Ishimaru, S., Arai, S., Ishida, Y., Shirasaka, M. and Okrugin, V.M. (2007) Melting and multi-stage metasomatism in the mantle wedge beneath a frontal arc inferred from highly depleted peridotite xenoliths from the Avacha volcano, southern Kamchatka. Journal of Petrology 48, 395-433.

Makeyev, A.B. (2006) Typomorphic features of Cr-spinel and mineralogical prospecting guides for Cr ore mineralization. Russian Journal of Earth Sciences, 8, ES3002, doi:10.2205/2006ES000196.

Morishita, T., Ishida, Y. and Arai, S. (2005) Simultaneous determination of multiple trace element compositions in thin (<30 μm) layers of BCR-2G by 193 nm ArF excimer laser ablation-ICP-MS: implications for matrix effect and elemental fractionation on quantitative analysis. Geochemical Journal, 39, 327-340.

Nicholls, I.A. (1974) A direct fusion method of preparing silicate rock glasses for energy-dispersive electron microprobe analysis. Chemical Geology, 14, 151-157.

Scherbakova, S.V. (1975) Mineralogy of ruby-containing metasomatic rocks in the Polar Urals (in Russian).

Shmelev, V.R. (2011) Mantle ultrabasites of ophiolite complexes in the Polar Urals: petrogenesis and geodynamic environments. Petrology, 19, 618-640.

Shmelev, V.R., Perevozchikov, B.V. and Moloshag, V.P. (2014) The Rai-Iz ophiolite massif in the Polar Urals: geology and chromite deposits. pp. 44, Field Trip Guidebook, 12th International Platinum Symposium, Yekaterinburg, IGG UB RAS.

Simonet, C., Fritsch, E. and Lasneir, B. (2008) A classification of gem corundum deposits aimed towards gem exploration. Ore Geology Reviews 34, 127-133.

Sun, S.-s. and McDonough, W.F. (1989) Chemical and isotopic systematics of oceanic basalts implications for mantle composition and processes. In Magmatism in the Ocean Basin, (Saunders, A.D. and Norry, M.J., Eds.). Geological Society Special Publication 42, 313-345.

Tropper, P. and Manning, C.E. (2004) Paragonite stability at 700 °C in the presence of H_2O-NaCl fluids: constraints on H_2O activity and implications for high pressure metamorphism. Contributions to Mineralogy and Petrology, 147, 740-749.

Manuscript received October 21, 2014
Manuscript accepted January 27, 2015
Published online March 19, 2015
Manuscript handled by Masaaki Obata